Interaction of ^{125}I-Labeled Botulinum Neurotoxins with Nerve Terminals. I. Ultrastructural Autoradiographic Localization and Quantitation of Distinct Membrane Acceptors for Types A and B on Motor Nerves

Jennifer D. Black and J. Oliver Dolly

Department of Biochemistry, Imperial College, London SW7 2AZ, United Kingdom. Dr. Black's present address is Grace Cancer Drug Center, Roswell Park Memorial Institute, New York State Department of Health, Buffalo, New York 14263

Abstract. The labeling patterns produced by radioiodinated botulinum neurotoxin (^{125}I-BoNT) types A and B at the vertebrate neuromuscular junction were investigated using electron microscopic autoradiography. The data obtained allow the following conclusions to be made. (*a*) ^{125}I-BoNT type A, applied in vivo or in vitro to mouse diaphragm or frog cutaneous pectoris muscle, interacts saturably with the motor nerve terminal only; silver grains occur on the plasma membrane, within the synaptic bouton, and in the axoplasm of the nerve trunk, suggesting internalization and retrograde intra-axonal transport of toxin or fragments thereof. (*b*) ^{125}I-BoNT type B, applied in vitro to the murine neuromuscular junction, interacts likewise with the motor nerve terminal except that a lower proportion of internalized radioactivity is seen. This result is reconcilable with the similar, but not identical, pharmacological action of these toxin types. (*c*) The saturability of labeling in each case suggested the involvement of acceptors; on preventing the internalization step with metabolic inhibitors, their precise location became apparent. They were found on all unmyelinated areas of the nerve terminal membrane, including the preterminal axon and the synaptic bouton. (*d*) Although ^{125}I-BoNT type A interacts specifically with developing terminals of newborn rats, the unmyelinated plasma membrane of the nerve trunk is not labeled, indicating that the acceptors are unique components restricted to the nerve terminal area. (*e*) BoNT types A and B have distinct acceptors on the terminal membrane. (*f*) Having optimized the conditions for saturation of these binding sites and calibrated the autoradiographic procedure, we found the densities of the acceptors for types A and B to be ~150 and 630/μm^2 of membrane, respectively. It is proposed that these membrane acceptors target BoNT to the nerve terminal and mediate its delivery to an intracellular site, thus contributing to the toxin's selective inhibitory action on neurotransmitter release.

BOTULINUM toxins, produced by the anaerobic bacterium *Clostridium botulinum* in several antigenically different but structurally related forms, are the most neurotoxic agents known, and are responsible for the neuroparalytic condition, botulism (reviewed in reference 39). Although many of these toxins occur in association with other protein(s) that exhibit haemagglutinin activity, the isolated neurotoxic protein has a molecular weight of ~150,000 and normally consists of two heterologous polypeptides (~100,000 and ~50,000). The unique toxicity of both the free botulinum neurotoxin (BoNT)[1] (4, 37, 38, 42, 43) and its complex (5) is attributable to their ability to inhibit irreversibly the spontaneous and evoked release of acetylcholine at peripheral synapses. The specificity of this action on the nerve terminal is highlighted by the absence of measurable effects on any other parameters (6, 18). Therefore, BoNT may prove useful for the identification of functional membrane components on motor nerves and in the elucidation of cellular processes concerned with transmitter release.

Light-microscopic autoradiographic studies have shown that ^{125}I-labeled BoNT type A binds specifically (7, 22) and saturably (7) to components of the neuromuscular junction in mouse diaphragm. The degree of resolution at the level of the light microscope, however, did not permit precise localization of the label in the synaptic region. Ultrastructural studies were necessary to distinguish between pre- and postsynaptic labeling and to establish whether the neurotoxin was associated with the membrane and/or intracellular targets. Using a radioiodinated derivative of BoNT type A (^{125}I-BoNT) that exhibits a high level of neurotoxicity (46), direct evidence for the saturable interaction of BoNT type A solely with the motor nerve terminal was presented for the first time (8). When nerve–muscle preparations were treated with this neurotoxin in vitro, under conditions known to block neurotransmission (2), resulting autoradiograms showed a dis-

1. *Abbreviations used in this paper*: BoNT, botulinum neurotoxin; ^{125}I-BoNT, radioiodinated BoNT; LD_{50}, amount of toxin that killed 50% of injected mice within 4 d.

tinct deposition of silver grains at motor nerve endings. The labeling was not restricted to the plasma membrane of the synaptic bouton, as silver grains were also present within the terminal cytoplasm. This finding was consistent with the suggestion (38) that the toxin's neuroparalytic action involves a target site within the nerve terminal.

It is important to note that the acceptors for the toxin were found (8) to be distributed uniformly on all areas of the synaptic bouton membrane; i.e., they were not restricted to the active zones where neurotransmitter release is thought to occur (21). However, it is not known whether these membrane acceptors are unique to the terminal membrane or if they are also present on the myelinated axon. Furthermore, in relation to the basis of BoNT-induced neuroparalysis, it is of interest to obtain ultrastructural evidence for the proposed transport of BoNT (15) along the nerve trunk. It needs to be established whether BoNT type A and type B, similar in structure and overall pharmacological action (cf. references 37, 39, and 41), share common neuronal acceptors at the neuromuscular junction.

In this study, distinct populations of acceptors for ^{125}I-BoNT types A and B were localized on all areas of the unmyelinated motor nerve terminal using electron microscopic autoradiography. Moreover, the density of these acceptors was determined after conditions for their saturation had been established; their role in targeting BoNT to cholinergic nerve terminals and in mediating the subsequent internalization is discussed with respect to the molecular basis of botulism.

Materials and Methods

Radioiodination of Neurotoxins and Bovine Serum Albumin (BSA)

BoNT types A and B were purified and radiolabeled by Dr. R. Williams of this laboratory (43, 46). Radioiodination was carried out using the chloramine-T method of Greenwood et al. (13), with important modifications. The ^{125}I-labeled preparations were of high specific radioactivity (450–1,700 Ci/mmol) and retained 60–85% of the neurotoxicity of native toxin preparations (representing 2×10^8 and 1.1×10^8 of the amount of toxin that killed 50% of injected mice in 4 d (LD_{50})/mg for types A and B, respectively). BSA was radioiodinated in a similar manner; after accurate determination of its specific radioactivity, it was used as a standard for measuring the efficiency of the autoradiographic procedure.

Tissue Labeling

In vivo studies. Mice were injected intraperitoneally with ^{125}I-BoNT type A (1 μg, equivalent to 8.8×10^4 mouse LD_{50} in 100 μl phosphate-buffered saline (PBS)/1% BSA; after death due to respiratory failure (~2 hr after injection), the paralyzed diaphragm was excised, washed, and processed for electron microscopic autoradiography as detailed below.

In vitro studies. Small pieces of mouse diaphragm tissue were incubated with ^{125}I-BoNT type A or B in 0.5 ml Krebs-Ringer's solution (124 mM NaCl, 5 mM KCl, 0.75 mM $CaCl_2$, 10 mM glucose, 1.3 mM $MgSO_4$, 1.2 mM KH_2PO_4, and 20 mM Na_2HPO_4, previously gassed for at least 30 min with 95% O_2/5% CO_2 and adjusted to pH 7.4) for 90 min at 22°C before extensive washing in Krebs-Ringer's solution at 4°C (five times, 6 min each) and fixation with 2% glutaraldehyde in the latter solution. After brief washing, the endplate regions were dissected, cut into small sections (~1 × 0.5 mm), and treated with 1% OsO_4 for 1 h, before being dehydrated in ethanol and embedded in Spurr's resin. Cutaneous pectoris muscle from a frog was processed similarly except that amphibian Ringer's solution (116 mM NaCl, 2 mM KCl, 2 mM $CaCl_2$, 0.5 mM NaH_2PO_4, 3mM glucose, and 5 mM Hepes [pH 7.2]) was used for the incubations and washes. Control samples were treated as above except that a 50–100-fold excess of native BoNT type A or B was included in the incubation medium.

To examine the basis of toxin internalization, mouse diaphragm tissue was pretreated with 15 mM Na azide and labeling with ^{125}I-BoNT types A and B was then examined. Concentration dependence of toxin binding was studied by incubating small pieces of the tissue with increasing concentrations of ^{125}I-BoNT (1.5–150 nM) for 90 min at 22°C, while the time course was investigated by labeling with type A radiolabeled toxin for various times (20–150 min), followed by the standard processing for microscopy. The distribution of acceptors for ^{125}I-BoNT type A along the motor nerve axon was investigated using the diaphragm of newborn rats, because the motor nerve is unmyelinated at this stage in development. The interaction of the different toxin types (A and B) at the motor nerve terminal was studied by pretreating the tissue with unlabeled toxin of one type for 1 h at 22°C followed by incubation with labeled toxin of the other type (for 90 min).

Electron-microscopic Autoradiography

Autoradiograms were prepared essentially by the method of Salpeter and Bachmann (33). Ultrathin sections of pale gold interference color were cut using an ultramicrotome (LKB Instruments, Inc., Gaithersburg, MD) and transferred to formvar-coated slides with a platinum wire loop. At least six groups of three to five test sections from a minimum of two different blocks were placed along one side of the slide and at least three groups of two to three control sections were arranged on the other. This ensured that all sections were exposed under the same conditions. The slides were then dipped in Ilford L4 nuclear emulsion (10 g in 24 ml) at 32°C using a semiautomatic coating device; the speed of withdrawal was adjusted to give a monolayer of crystals with a purple interference color (~170 nm thick). Slides were exposed for 3–6 wk at 4°C in light-tight plastic slide boxes. The emulsion was then developed in Kodak D-19 developer, fixed in 25% sodium thiosulphate, and the formvar film was stripped off onto the surface of distilled water. Sections were picked up with parafilm and stained with 12% uranyl acetate for 20 min before being viewed in a Hitachi-600 electron microscope.

Quantitation

For comparison of the extent of labeling under different conditions, 25–35 endplates from each preparation were photographed at a magnification of 10,000 and prints were prepared at a final magnification of 20,000. The thickness of the sections was measured by Small's method (40), using appropriate folds in the sections; only those of similar thickness were used for quantitative studies. The membrane enclosing the synaptic boutons was traced onto acetate sheets and its length measured in micrometers using a digitizer (Hewlett-Packard Co., Palo Alto, CA). Grains were then counted and expressed per unit length of presynaptic membrane.

Absolute Quantitation of Acceptors for ^{125}I-BoNT Types A and B

Acceptors were quantitated by the method of Fertuck and Salpeter (11). Nerve–muscle preparations were treated with saturating concentrations of type A or B ^{125}I-BoNT for 90 min at 22°C to ensure total occupancy of specific sites at the motor nerve terminal. After small samples of the endplate regions were processed for microscopy, at least nine groups of three to five pale gold tissue sections from different blocks containing large numbers of nerve endings were arranged on each slide. After exposure periods ranging from 1 to 6 wk, the emulsion was developed and the stained sections viewed in the electron microscope. Nerve terminals from sections of similar thickness only were photographed and prints prepared at a magnification of 28,300. The density of acceptors was determined using the following equation (11):

$$\text{sites}/\mu m^2 = \frac{G \times D}{124{,}800\ (1 - e^{-0.01155t})} \times \frac{A}{S_0 C},$$

where G is the grain density (No. grains/μm^2 membrane), D is the decays required for one developed grain (or 1/percent efficiency), t is the exposure time in days, A is Avogadro's number (6.023×10^{20} molecules/mmol), S_0 is the specific activity of the radiolabeled toxin at the beginning of the exposure period (curies per millimole), and C is the disintegrations per minute or 2.22×10^{12}. Grain density was determined by measuring the length of the presynaptic membrane in micrometers by digitization and counting the silver grains along its length. The percent efficiency of the autoradiographic technique used was determined by processing sections of ^{125}I-BSA of known radioactivity for electron microscopic autoradiography and developing the emulsion after different exposure periods (34). The number of grains produced per radioactive decay could then be calculated.

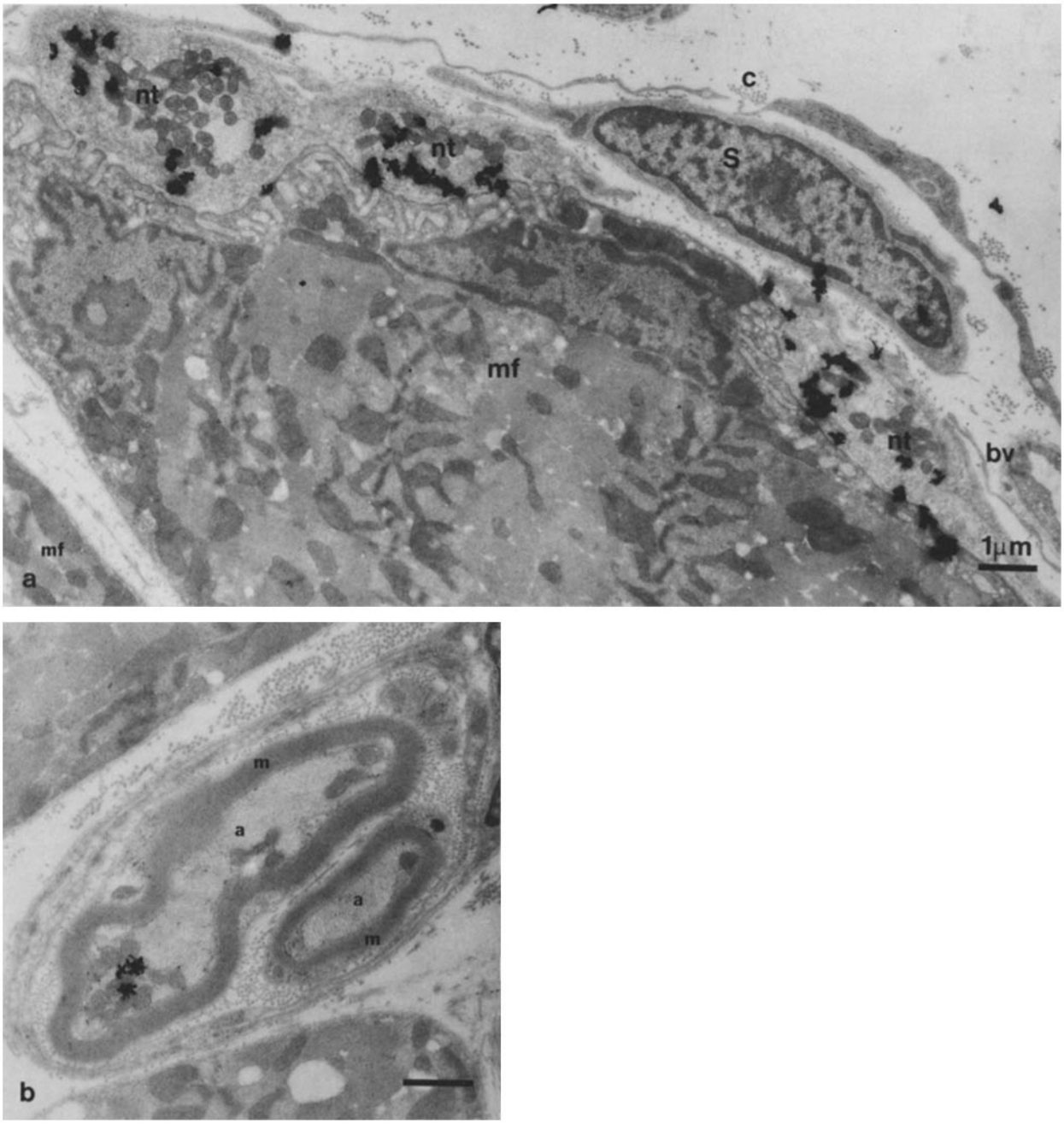

Figure 1. Interaction of ^{125}I-BoNT type A with motor nerves after in vivo administration to mice. (*a*) Motor nerve terminals (*nt*) labeled with ^{125}I-BoNT type A after intraperitoneal injection of ~1 μg of radioiodinated toxin (in 100 μl PBS/1% BSA) into a mouse. Autoradiograms were developed after 3-wk exposure. Note the absence of silver grains on muscle fibers (*mf*), Schwann cells (*S*), blood vessels (*bv*), and collagen (*c*). (*b*) Transverse section through a myelinated axon from a mouse diaphragm treated as above. Grains are seen in the axoplasm (*a*) but no labeling of the protective myelin sheath (*m*) is observed.

Results

Labeling Profiles for ^{125}I-BoNT Types A and B in Mouse Diaphragm and Frog Cutaneous Pectoris Muscle

Sections of mouse diaphragm tissue labeled with ^{125}I-BoNT type A in vivo showed deposition of silver grains at the motor nerve terminal (Fig. 1 *a*). No labeling of muscle fibers, Schwann cells, blood vessels, collagen fibrils, or myelin was detected in any of the sections, emphasizing the specificity of the interaction of radiolabeled BoNT type A with the motor nerve terminal. At the labeled nerve terminals, grains were observed both on the presynaptic plasma membrane and within the cytoplasm, indicating the involvement of an internalization step (Fig. 1 *a*). Most of the developed grains (63% of the total) were on the membrane (Table I) and could be seen on all areas of the unmyelinated nerve terminal (see below). Moreover, silver grains were observed within the

Table I. Distribution of Silver Grains at Motor Nerve Terminals Labeled under Different Conditions with ^{125}I-BoNT Types A and B

Labeling conditions	Na Azide (15 mM)	Distribution of grains with respect to the plasma membrane % of total	
		On	Inside
In vivo			
^{125}I-BoNT type A(~1 μg)	−	63	37
In vitro			
^{125}I-BoNT type A(15 nM)	−	62	38
^{125}I-BoNT type A(11 nM)	+	100	−
^{125}I-BoNT type B(10 nM)	−	75	25
^{125}I-BoNT type B(20 nM)	+	100	−

Large numbers (20–50) of nerve endings from mouse diaphragm preparations treated with ^{125}I-BoNT in vivo (after intraperitoneal injection of the mouse) or in vitro (in Krebs-Ringer's solution for 90 min at 22°C), using the conditions specified, were processed for electron microscopic autoradiography (as detailed in Materials and Methods) and photographed. When Na azide was included (+), the samples were preincubated for 30 min before addition of BoNT. The silver grains on the nerve membrane and inside the synaptic bouton were counted independently and expressed as percent of the total. A grain was considered to be on the membrane if it was located within 60–70 nm of the plasma membrane.

axoplasm of myelinated axons, suggesting that retrograde intra-axonal transport had occurred (Fig. 1 *b*).

A similar pattern of labeling was observed in sections from samples treated with 15 nM ^{125}I-BoNT type A in vitro, thus confirming the validity of the in vitro model for localization studies (Fig. 2 *a*). Silver grains were observed only at the unmyelinated motor nerve terminals; these occurred both on the plasma membrane (62%) and within the terminal (38%) (Table I). The internalized radioactivity did not appear confined to any particular intraterminal compartment, although grains were sometimes seen associated with the membrane of vacuolar structures. Control sections, treated with ^{125}I-BoNT type A in the presence of excess native neurotoxin, were virtually devoid of silver grains (Fig. 2 *b*); native BoNT reduced the extent of labeling to 4% of that seen in test samples. Collectively, these results showed that the interaction of ^{125}I-labeled type A toxin with its target tissue was both selective and saturable, thus demonstrating the involvement of acceptors. Saturable labeling of the neuromuscular junction was also observed using light-microscopic autoradiography after incubation of the tissue with 0.2 nM ^{125}I-BoNT type A, a concentration in the range of that required for neuroparalysis in vitro (38), but too low to allow detection in ultrathin sections. Where autoradiography was combined with histochemical localization of acetylcholinesterase (7, 44) (to label the neuromuscular junction), silver grain clusters coincided with areas reacting with acetylthiocholine (data not shown).

^{125}I-BoNT type B also interacted specifically and saturably with the motor nerve terminal (Fig. 2, *c* and *d*). After 11-d exposure, grains were deposited both on the plasma membrane and within the synaptic bouton itself, suggesting that uptake of toxin had taken place, as previously observed with type A, except that the extent of internalization was considerably less (Table I). As found with A, intraterminal grains were often associated with vacuole-like structures (Fig. 2 *c*); likewise, the presence of silver grains within myelinated axons suggested retrograde axonal transport of radioactivity had taken place (data not shown).

A similar pattern of labeling was also observed with frog cutaneous pectoris (Fig. 3); silver grains were observed both on the membrane and in the cytoplasm of test sections labeled with ^{125}I-BoNT type A, while controls were completely devoid of silver grains, indicating saturability of the binding (data not shown). The extent of labeling at the amphibian nerve terminal was, however, considerably less than in mammalian tissue; this difference is reconcilable with the apparent lower sensitivity of frog muscle to the action of the toxin (31).

Interaction of Types A and B Botulinum Neurotoxins

Preincubation of a mouse nerve-hemidiaphragm with a 100-fold excess of type B neurotoxin did not prevent binding or internalization of ^{125}I-BoNT type A at the motor nerve terminal (Fig. 4 *a*). Quantitative analysis of resultant autoradiograms (see Materials and Methods) showed that the number of grains per micrometer of plasma membrane was the same in sections incubated with ^{125}I-BoNT type A in the presence and absence of unlabeled type B (Table II).

In the converse experiment, type A did not prevent completely the binding of ^{125}I-BoNT type B, as silver grains were still seen at terminals preincubated with unlabeled type A neurotoxin (Fig. 4 *b*). However, quantitation of the data obtained demonstrated that specimens exposed to ^{125}I-BoNT type B in the presence of type A showed a 24% reduction in the extent of labeling relative to those treated with radioiodinated type B alone (Table II). Thus, in contrast to the lack of antagonism seen when terminals were labeled with ^{125}I-BoNT type A in the presence of type B BoNT, this partial inhibition suggests that type A interacts indirectly with at least some of the acceptors for type B.

Localization of Acceptors for ^{125}I-BoNT Types A and B at the Murine Motor Nerve Terminal

Although the saturability of the labeling of motor nerve terminals with ^{125}I-BoNT in vitro implicated membrane acceptors, their exact location was not apparent due to masking by grains resulting from internalized radioactivity. As detailed in the accompanying report (2), the internalization step can be prevented totally using inhibitors of energy production (such as Na azide and dinitrophenol) and by low temperature (e.g., 4°C); this allows the interaction of the radiolabeled toxins with their acceptors to be examined.

In the presence of 15 mM Na azide, radioactivity seemed to occur solely on the plasma membrane (Fig. 5, *a* and *b*; Table I); nonspecific labeling was minimal (data not shown). To ensure that the nerve terminal membrane was indeed the source of the silver grains (particularly those opposite the postsynaptic folds [29]), quantitative studies were carried out as follows (35): the distance from the midpoint of at least 500 silver grains to the plasma membrane was measured and used to construct a grain-density distribution histogram. As Fig. 6 *a* shows, the distribution was bell-shaped, indicating that the majority of grains were found on the terminal membrane or very close to it. Since the scatter is symmetrical on both sides of the "biological line source," the presence of acceptors on the postsynaptic plasma membrane can be ex-

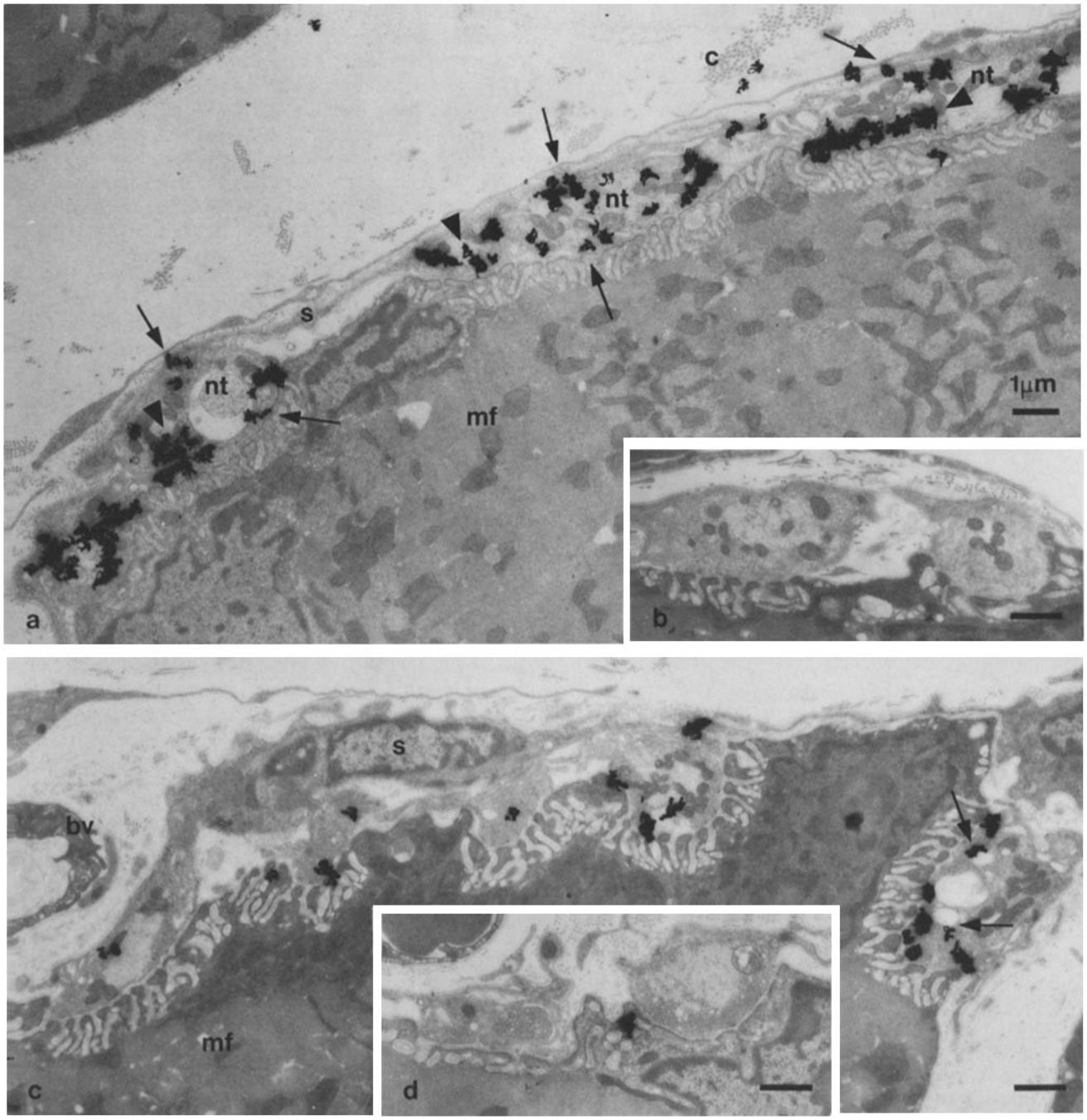

Figure 2. Interaction of ^{125}I-BoNT types A and B with the murine motor nerve terminal in vitro detected by electron microscopic autoradiography. (*a*) Motor endplate from a mouse diaphragm treated with ^{125}I-BoNT type A (15 nM). Sections were exposed for 3 wk. Silver grains are seen on the nerve terminal membrane (*arrows*) and in the cytoplasm (*arrowheads*). (*b*) Control preparation treated as described in *a* in the presence of a 100-fold excess of unlabeled BoNT type A. (*c*) Five synaptic boutons from a nerve–muscle preparation treated with ^{125}I-BoNT type B (10 nM) and exposed for 11 d. Note the presence of silver grains on the presynaptic plasma membrane and within the cytoplasm where they are often associated with the membrane of vesicular structures (*arrows*). (*d*) Control nerve terminals treated with ^{125}I-BoNT type B in the presence of excess (100-fold) unlabeled toxin showed ~1% of the labeling seen in test sections indicating that, as in *a*, the interaction is saturable. See Fig. 1 legend for explanation of symbols.

cluded. The half-distance value, i.e., the distance from a radioactive line within which half of the developed grains are located, was determined from the integrated grain distribution histogram shown in Fig. 6 *b*, and found to be ~56 nm. At a distance of only 100 nm, the number of grains was very low, indicating that the autoradiographic method used gives good resolution.

The saturable acceptors for both toxin types were not restricted to the active zones but extended uniformly to all the unmyelinated terminal arborizations of the nerve as far as the

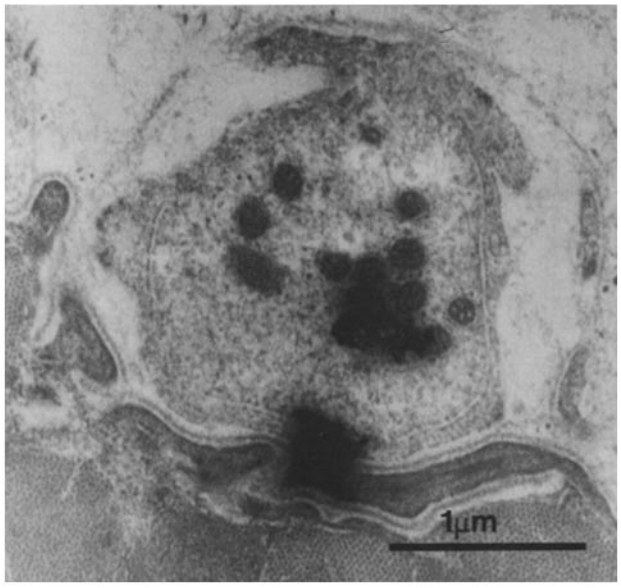

Figure 3. Binding and internalization of ^{125}I-BoNT type A at the amphibian neuromuscular junction. Cross section of a nerve terminal from frog cutaneous pectoris tissue incubated with 15 nM ^{125}I-BoNT type A in amphibian Ringer's solution. The pattern of labeling is similar to that at the mammalian nerve terminal; silver grains are observed on the presynaptic membrane and within the cytoplasm.

terminal node of Ranvier (Fig. 7, *a–c*). No grains were detectable on the protective myelin sheath, but the possibility of specific acceptors also occurring on the plasma membrane of the myelinated axons (to which toxin molecules had no access) could not be excluded. As the motor neurons innervating the diaphragm of newborn rats are still unmyelinated at this stage of development (47) and the Schwann cells that loosely surround the axons do not appear to prevent toxin molecules from reaching the axonal plasma membrane, the possible distribution of acceptors on the axon could be evaluated in this preparation. Newborn rats are highly susceptible to intoxication by ^{125}I-BoNT type A, dying within a few hours of an intraperitoneal injection of low (<1 LD_{50} for adult mice) doses of the toxin. Accordingly, saturable binding of ^{125}I-BoNT type A was detected at the developing motor nerve terminals in test sections (Fig. 8, *a* and *b*); control autoradiograms were completely devoid of silver grains (Fig. 8 *c*). Although a few grains were present on the axonal areas nearest the developing terminal matrices, no labeling was apparent in the large bundles of unmyelinated axons more distant from the terminal regions (Fig. 8 *d*). These observations suggest that the acceptors are located only in those areas of the axonal plasma membrane not destined to become myelinated, i.e., the terminal areas. Most of the nerve terminals observed were too small to allow detection of internalization, but in those that were slightly larger uptake was apparent (Fig. 8 *b*).

Density of Acceptors for ^{125}I-BoNT Types A and B on the Unmyelinated Nerve Terminal Membrane

Optimization of conditions for saturation of specific acceptors with ^{125}I-BoNT. Inhibition of the internalization step of intoxication by ^{125}I-BoNT types A and B using metabolic inhibitors permitted the absolute quantitation of their acceptors at the nerve terminal. To carry out such determinations, it was essential to establish the toxin concentration and incubation period required to saturate the sites for each toxin type. Saturation of the acceptors in the presence of azide was achieved using 15 nM ^{125}I-BoNT type A for 90 min at 22°C (Table III). A significant amount of radioactivity was seen associated with motor nerve terminals after only 20 min (84% of maximum binding, see Table III); maximum binding was attained by 90 min with this toxin concentration, despite the restricted diffusion into this tissue (1).

In the case of ^{125}I-BoNT type B (Table III), the labeling observed using 20- and 100-nM concentration (for 90 min at 22°C) did not differ appreciably; for quantitative studies, 100 nM was used to ensure saturation.

Calibration of the autoradiographic technique. To determine the percent efficiency (32) of the method used routinely, ultrathin sections containing a known amount of radioactivity (in the form of ^{125}I-labeled BSA) were processed for autoradiography and developed after varying lengths of time. A linear increase was observed (Fig. 9 *a*) in the number of silver grains produced during the first 3-wk exposure; longer exposure times, however, resulted in a slight leveling of the curve. Percent efficiency (Fig. 9 *b*) decreased from ~63% (almost maximum; see reference 32) for the shortest exposure time (4 d) to 57% for the longest (42 d), the average being 60 ± 3.2% (n = 6). The background grain density, obtained by photographing random areas of the sections that did not contain ^{125}I-labeled BSA, was negligible.

To ensure that 60% efficiency was applicable to test specimens incubated with ^{125}I-BoNT, groups of sections from samples that had been previously saturated with ^{125}I-BoNT type A and processed for electron microscopic autoradiography were developed each week for 6 wk. The number of grains per micrometer of plasma membrane was then determined for each exposure time and expressed as a function of time (Fig. 10). The plots obtained for ^{125}I-BSA and ^{125}I-BoNT type A were very similar and 60% was considered a valid estimate of the efficiency in this system.

Acceptor densities. The average number of acceptors for BoNT type A was 152(± 20%)/μm² of membrane when 150 nM ^{125}I-BoNT and 7–42-d exposure were used (Table

Table II. Interaction of Types A and B BoNT at Motor Nerve Terminals

Incubation conditions	Number of grains per micrometer plasma membrane
^{125}I-BoNT type A (15 nM)	0.67 (100%)
Type B BoNT (1.5 μM) + ^{125}I-BoNT type A (15 nM)	0.71 (106%)
^{125}I-BoNT type B (10 nM)	1.10 (100%)
Type A BoNT (1 μM) + ^{125}I-BoNT type B (10 nM)	0.84 (76%)

Samples of mouse diaphragm tissue were preincubated in Krebs-Ringer's solution with unlabeled toxin of one type (A or B) for 1 h at 22°C before the addition of radioiodinated toxin of the other. Incubation was carried out for 90 min (at 22°C), followed by washing and routine processing for autoradiography. After 3-wk exposure, the sections were viewed in the electron microscope and ~20–30 endplates from each preparation were photographed. The total length of presynaptic membrane seen in the prints was measured by digitization; the number of grains associated with the nerve terminals was determined and grain density was calculated for each preparation. This allowed the labeling observed under different conditions to be compared quantitatively.

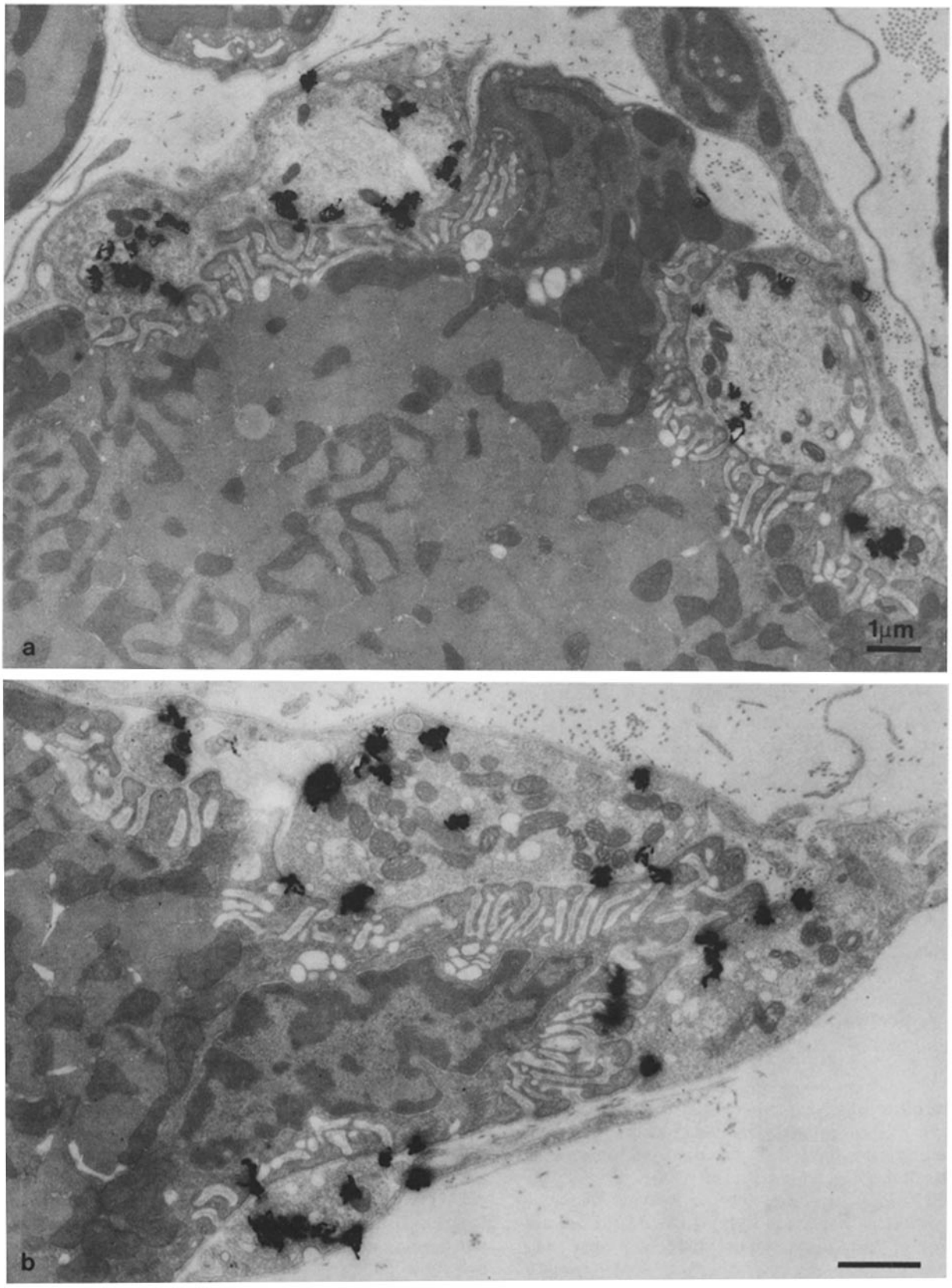

Figure 4. Interaction of types A and B BoNT at the murine motor nerve terminal. (*a*) Cross-sectional view of four synaptic boutons labeled with ^{125}I-BoNT type A in the presence of unlabeled type B BoNT. The tissue was preincubated with type B BoNT (1.5 μM) for 1 h at 22°C before incubation for 90 min with radiolabeled type A, at a final concentration of 15 nM. (*b*) Section of a motor endplate pretreated with unlabeled type A BoNT (1 μM) for 1 h at 22°C followed by addition of ^{125}I-BoNT type B to a final concentration of 10 nM, with further incubation for 90 min. Silver grains are present at the nerve terminals, but labeling is somewhat less extensive than that observed in control specimens.

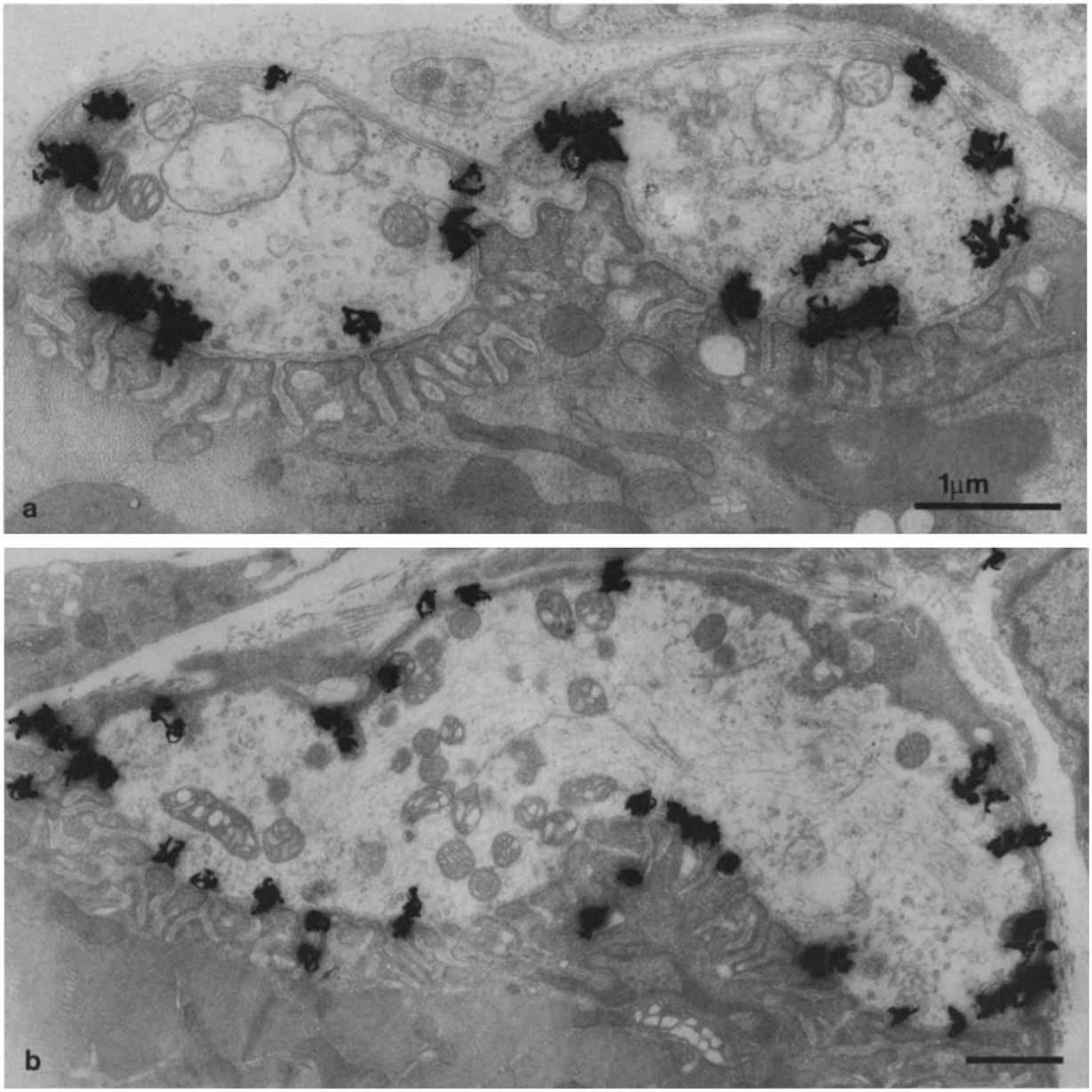

Figure 5. Localization of acceptors for ^{125}I-BoNT types A and B at the murine motor nerve terminal. Nerve–muscle preparations were treated with Na azide (15 mM) for 30 min at 22°C before a 90-min incubation with ^{125}I-BoNT type A or B, in the presence of the metabolic inhibitor. Autoradiograms of samples treated (*a*) with ^{125}I-BoNT type A (150 nM) or (*b*) with type B (20 nM).

IV). When quantitation of acceptors was performed using 15 and 35 nM ^{125}I-BoNT type A, similar numbers were obtained, confirming that these concentrations do, in fact, saturate the binding sites (Table III). The density of ^{125}I-BoNT type B sites was determined, likewise, by processing two different blocks of diaphragm tissue (treated with 100 nM ^{125}I-BoNT type B, see above) for electron microscopic autoradiography. Using an efficiency value of 62% (more appropriate for the exposure used), the average site density was 627 ± 21% (the range of values being 495–759; Table IV). Hence, the density of sites for ^{125}I-BoNT type B is approximately four times greater than that for A.

Discussion

The grain distribution in autoradiograms of mouse diaphragm labeled in vivo with ^{125}I-BoNT type A using a concentration (extrapolated) of <3 nM was indistinguishable from that seen after in vitro labeling with 1.5 nM (or higher); this emphasizes the validity of the latter as a means for observing labeling patterns that are relevant to BoNT poisoning. Moreover, the presence of silver grains in the axoplasm of myelinated nerves demonstrates that the toxin, or a portion of the molecule, undergoes retrograde intra-axonal transport as has been shown for tetanus toxin (30) and nerve growth

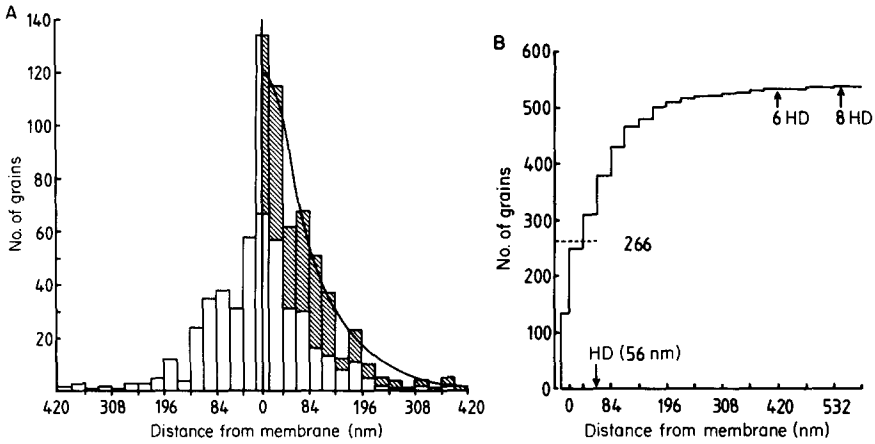

Figure 6. Histogram of experimental grain-density distribution around a radioactive line source: determination of the half-distance (HD) value (35). (*A*) The distance from a biological line source (i.e., the plasma membrane of motor nerve terminals treated with ^{125}I-BoNT type A in the presence of Na azide as described in Fig. 5) to the midpoint of >500 silver grains was measured and a histogram of grain-density distribution about the line was constructed with the data. Because this histogram appeared symmetrical on both sides (indicating that the source was in fact a line), a one-sided histogram (shaded bins) was also plotted. A smooth curve was then drawn in by eye. Most of the grains were located on or very close to the membrane, as reflected by the bell-shaped curve. (*B*) Following the method of Salpeter et al. (35), the results shown in *A* were used to plot an integrated grain distribution histogram. Each column gives the total number of grains within that distance from the source. The number of grains changed very little after ~300 nm and counting was stopped at a cut-off distance of ~600 nm. The half-distance value was determined readily from this histogram: the total number of grains is 532; half the total (i.e., 266 grains) can thus be found within ~56 nm of the source.

factor (19). The pathway for retrograde axonal transport of exogenous proteins usually begins with uptake by endocytosis at the nerve ending or unmyelinated portions of the preterminal axon (12). Protein is carried in the axon inside various vesicular or tubular organelles to the cell body where it may be transferred to lysosomes (25), to some other compartment in the cell, or by transsynaptic migration to presynaptic terminals that synapse on that cell body (e.g., tetanus toxin). The purpose for the neural ascent of BoNT is unknown; however, studies carried out by Hagenah et al. (16), in which toxin injected into muscle and allowed to ascend the motor nerve was found not to affect central cholinergic neurotransmission suggest that, unlike tetanus toxin, a (modified) inactive form is involved. Transport of BoNT to the cell body may be necessary for its degradation because the neuronal cell body is richer in both primary and secondary lysosomes than the axon and nerve endings (24).

The pattern of labeling with type B is comparable to that seen with A, in accordance with the related pharmacological action of these toxin types. However, although both neurotoxins appear to be internalized, the extent of uptake of B is appreciably lower (~40% less) than that of type A. If, as has been suggested previously (38), internalization of toxin is required for expression of toxicity, the demonstrable reduction in the proportion of translocated radioactivity could account for the lower toxicity of BoNT type B in mice.

Using the inhibitor of oxidative phosphorylation Na azide to prevent internalization of radioactivity, the exact location of the specific acceptors for ^{125}I-BoNT types A and B was established. Resolution studies confirm that these are indeed presynaptic and membrane-associated; this result is consistent with the lack of direct postsynaptic effects being induced by BoNT (36). In both cases, silver grains were uniformly distributed on all unmyelinated areas of the nerve terminal membrane; thus, the acceptors are not located solely in the synaptic region but also on preterminal axonal plasma membrane. Since the protective myelin sheath does not allow access of molecules to the axonal membrane it encloses, the presence of acceptors in areas beyond the terminal node of Ranvier was investigated in newborn rats. Myelination of motor neurons is incomplete at this stage of development (26), leaving the entire length of the nerve trunk exposed to the external environment. Saturable acceptors for ^{125}I-BoNT type A were found only on the terminal membrane of these immature synapses; large bundles of nerves destined to become myelinated were unlabeled. It appears, therefore, that the sites are restricted to the unmyelinated terminal arborizations of the motor nerve; a similar distribution was recently reported for α-latrotoxin binding sites except that only the synaptic bouton membrane, and not the preterminal axon, was labeled (45). It is interesting that types A and B BoNT do not appear to share common membrane acceptors at the nerve terminal. Further evidence for the presence of a distinct population of sites for each toxin type is given by their different densities. The absolute number of sites for the two toxin types represents the first direct measurement of the density of any component on the unmyelinated mammalian motor nerve terminal membrane. The number of sites per

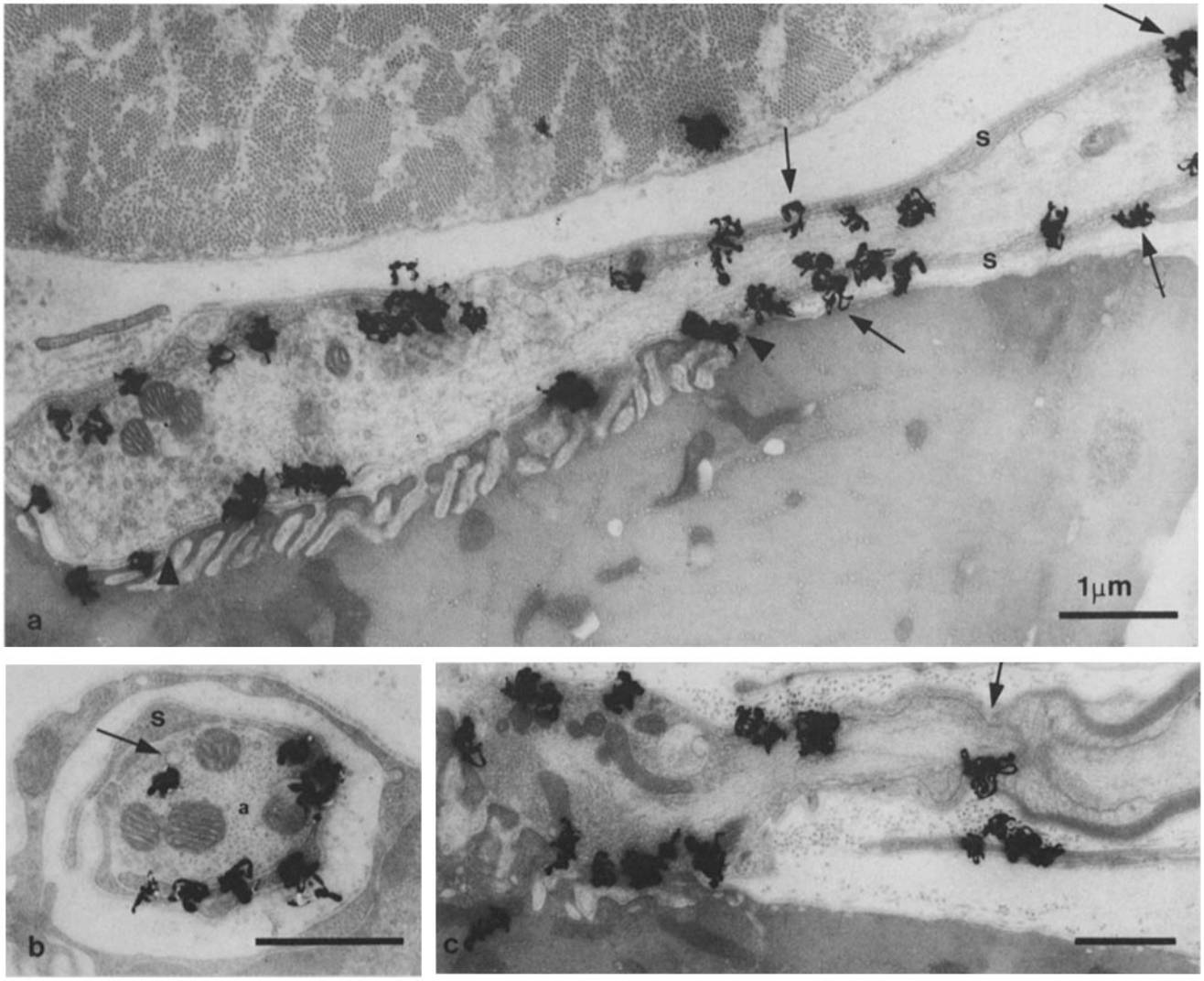

Figure 7. Saturable acceptors for ^{125}I-BoNT on the membrane of unmyelinated axons. (*a*) Autoradiogram of a longitudinal section through an unmyelinated axon and a synaptic bouton labeled with ^{125}I-BoNT type A in the presence of Na azide (15 mM). Silver grains are seen on the plasma membrane of the terminal axon (*arrows*). *S*, Schwann cell processes loosely surrounding the axon. *Arrowheads*, the area of the active zones, from which transmitter release is thought to occur. (*b*) Transverse section through an unmyelinated axon (*a*) which is surrounded loosely by Schwann cell processes (*S*). The tissue was treated with ^{125}I-BoNT type A (15 nM). Silver grains are seen associated with the axonal plasma membrane and also with intra-axonal vesicles (*arrows*). (*c*) Unmyelinated axon labeled with ^{125}I-BoNT type B (10 nM) right up to the terminal node of Ranvier (*arrow*). Note that in this preparation, which was treated in the absence of metabolic inhibitors, all silver grains are associated with the neuronal plasma membrane.

square micrometer of membrane for ^{125}I-BoNT types A and B is 153 ± 31 and 627 ± 131, respectively.

The acceptors studied autoradiographically appear to be involved in the action of the toxin because of the discrete and selective labeling patterns seen both in vivo and in vitro with BoNT concentrations in the range that blocks neurotransmission (38). Additional support for this deduction is provided by their demonstrated presence only at terminals (3) where BoNT effectively inhibits transmitter release (3, 8). Regarding the precise manner in which the acceptors participate in the neuroparalytic action of the neurotoxin, analogies are apparent with other bacterial and plant toxins in certain respects. As in the case of these other toxins (e.g., diphtheria toxin, tetanus toxin, abrin, ricin, and modeccin), BoNT acceptors may ensure that toxin is concentrated on the cell surface (for review, see reference 28) and directed to a particular intracellular vesicular compartment. In the light of the results presented here the theoretical "pipe and valve" model of Hanig and Lamanna (17), which suggests that the interaction of BoNT with surface acceptors is directly responsible for toxicity, does not seem a viable proposition. The acceptors for ^{125}I-BoNT types A and B, which appear to be distinct, are not restricted solely to the active zone areas opposite the postsynaptic folds (although the presence of a small number of higher affinity sites within the active zones has not been excluded). Furthermore, the calculated density of acceptors far exceeds the estimated number of 500 active zones per nerve terminal (20). Finally, it is difficult to reconcile

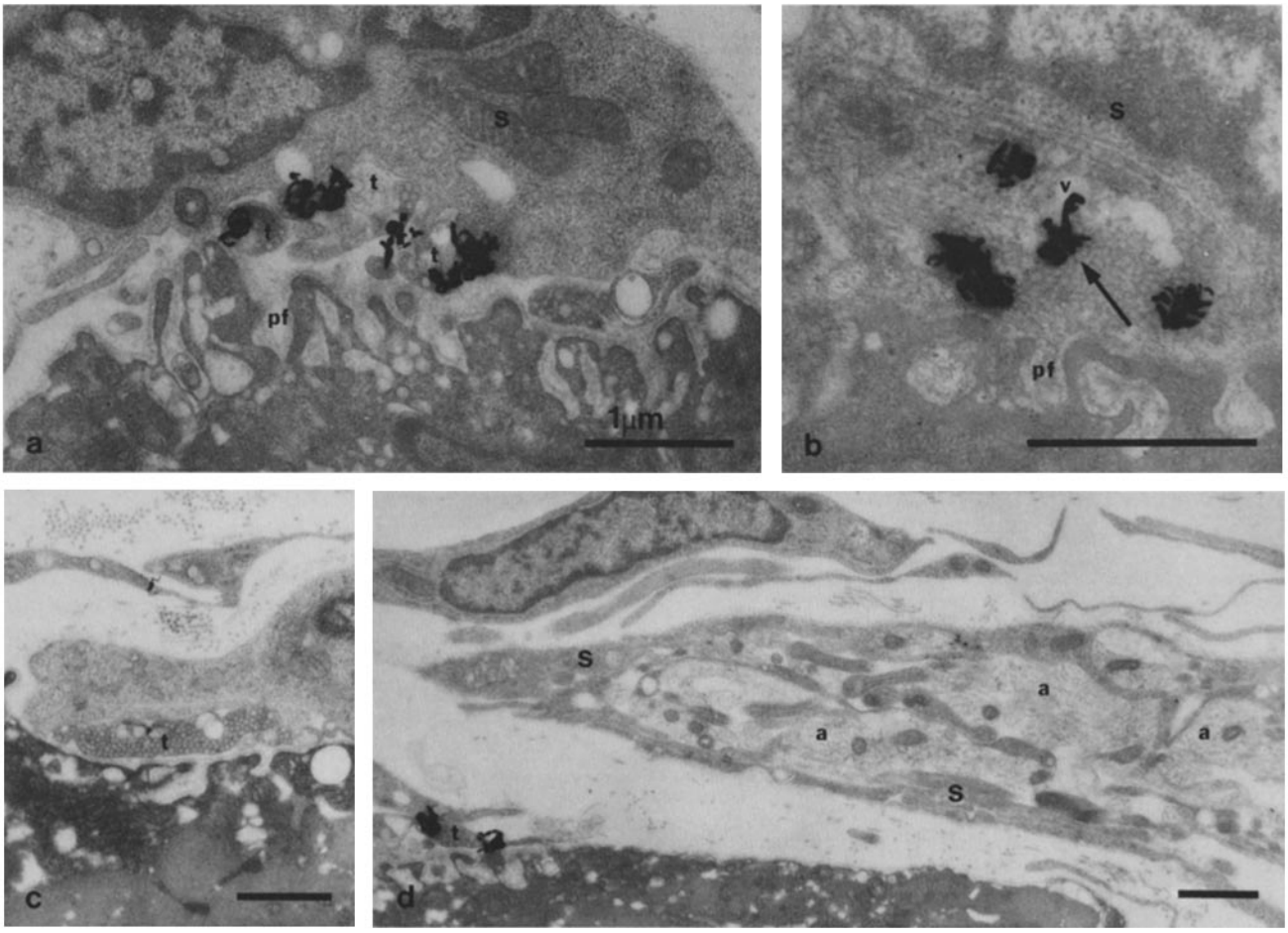

Figure 8. Interaction of ^{125}I-BoNT type A with the developing motor nerves of newborn rats. The diaphragm of a newborn rat was incubated with ^{125}I-BoNT (30 nM) in 0.5 ml Krebs-Ringer's solution for 90 min at 22°C, followed by extensive washing at 4°C. Sections processed for autoradiography were exposed for 4 wk. (*a*) Developing motor nerve terminals labeled with ^{125}I-BoNT. Note the postsynaptic folds (*pf*) in the muscle cell and the numerous small axon terminals (*t*) embedded in an overlying Schwann cell (*S*). (*b*) Larger nerve terminal from a newborn rat diaphragm labeled with ^{125}I-BoNT type A. Note the internalized silver grain (*arrow*) possibly associated with a vesicular structure (*v*), the overlying Schwann cell (*S*), and the postsynaptic folds in the muscle cell (*pf*). (*c*) Control nerve terminal (*t*) treated with radiolabeled BoNT in the presence of excess (3 μM) unlabeled toxin. (*d*) Unmyelinated axons (*a*) loosely wrapped by Schwann cells (*S*) in a newborn rat diaphragm preparation treated as described above. Although the nerve terminal (*t*) areas (*left*) are labeled with ^{125}I-BoNT, no silver grains are detectable on the unmyelinated axonal membrane.

this theoretical proposal with the apparent requirement for toxin internalization before expression of neurotoxicity (5, 38) and with the action of other toxins of similar overall structure. It does not appear, therefore, that BoNT acts by blocking physically the neurotransmitter release sites; of course, the possibility that toxin molecules interact with the active zones intracellularly remains likely. Another proposed model suggests that the toxin acts as a Ca^{++} channel blocker (23). The distribution of BoNT sites, however, does not correspond with that predicted for Ca^{++} channels from electron microscopic freeze-fracture studies (21). Moreover, the absence of binding sites for BoNT at adrenergic and several other synapse types (3, 8) would exclude the Ca^{++} channel as its possible acceptor, as this channel ought to be similar in, at least, some of the nerves studied. In accord with this, BoNT is known to be ineffective towards Ca^{++} currents measurable in presynaptic membranes (9, 14).

Regardless of the physiological function of the acceptors, their density is far too high to be reconcilable with the number of neurotoxin molecules needed to induce paralysis in vivo. For example, the LD_{50} for a mouse is $\sim 1.2 \times 10^{-11}$ g or 8×10^{-17} mol, equivalent to 5×10^7 molecules of BoNT type A. From this LD_{50}, it can be calculated that an absolute maximum of 10^2–10^3 molecules are required to induce blockade of neurotransmission at each synapse (calculated as described in reference 39). As the observed densities of acceptors are ~150 and 630/μm^2 of membrane for ^{125}I-BoNT types A and B, respectively, these greatly exceed the number of molecules needed to inhibit neurotransmitter release at a synapse. Thus, these autoradiographic data appear to dismiss totally a "one-hit" model for the mechanism of action of these BoNT types. This is further supported by the finding that, although types A and B have a similar pharmacological action at the neuromuscular junction, they do not appear to share acceptors on the neuronal membrane.

Collectively, our findings show that the acceptors are

Table III. Concentration Dependence and Time Course of the Binding of Types A and B ^{125}I-BoNT to Nerve Terminal Membranes

Toxin concentration (90 min)*	Number of grains per micrometer of plasma membrane‡ Type A	Type B
nM		
1.5	0.23 ± 0.03	–
10.0	–	0.53 ± 0.06
15.0	0.55 ± 0.06	–
20.0	–	0.81 ± 0.07
35.0	0.56 ± 0.06	–
100.0	–	0.95 ± 0.07
Incubation with 15 nM toxin*		
min		
20	0.46 ± 0.08	–
90	0.55 ± 0.06	–
150	0.53 ± 0.09	–

* Mouse diaphragms were preincubated in Krebs-Ringer's solution containing 15 mM Na azide for 30 min at 22°C followed by labeling with ^{125}I-BoNT type A or B in the latter solution, under the conditions specified above.
‡ After the standard processing for electron microscopic autoradiography, average grain densities were determined at a minimum of 25 endplates from several sections (of the same thickness) taken from different blocks of the tissue; these (± SE) are expressed (27) per unit length of presynaptic membrane.

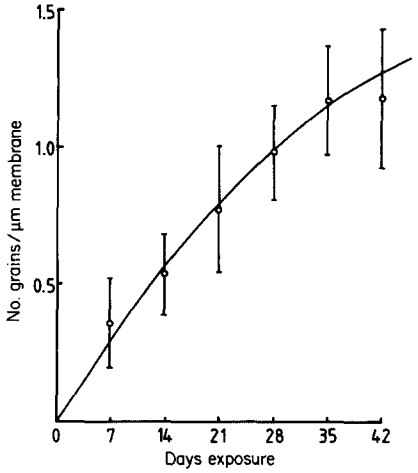

Figure 10. Time course of grain development on the nerve terminal membrane labeled with ^{125}I-BoNT. Sections of nerve terminals previously labeled with 150 nM ^{125}I-BoNT type A (in the presence of Na azide), were developed each week for 6 wk. 20–34 endplates (100–300 silver grains) were photographed for each time point. Grains were counted and the length of the nerve terminal membrane was determined by digitization. Grain density (number of grains per micrometer membrane) was then plotted as a function of exposure time; for quantitative analysis exposure times of 7–28 d are optimal.

responsible for targeting BoNT to motor nerve terminals where they mediate (2) internalization; this could facilitate inhibition of acetylcholine release by direct or indirect interaction of the toxin (or a fragment) with an intraterminal component concerned with the process. The large number of acceptors detectable, relative to the number of BoNT molecules required to cause neuroparalysis, should ensure an efficient delivery of toxin to its pharmacological target; this could be one contributory factor to its unique potency. Apart from being utilized by BoNT, these naturally occurring membrane components undoubtedly must serve some as yet unidentified function in their own right. Apparently, the BoNT types recognize determinants unique to cholinergic (3) nerve terminals, implicating them in some characteristic function. The toxins may thus prove to be powerful tools for investigations on the nature of these terminals; they may also provide insight into the differences between the unmyelinated

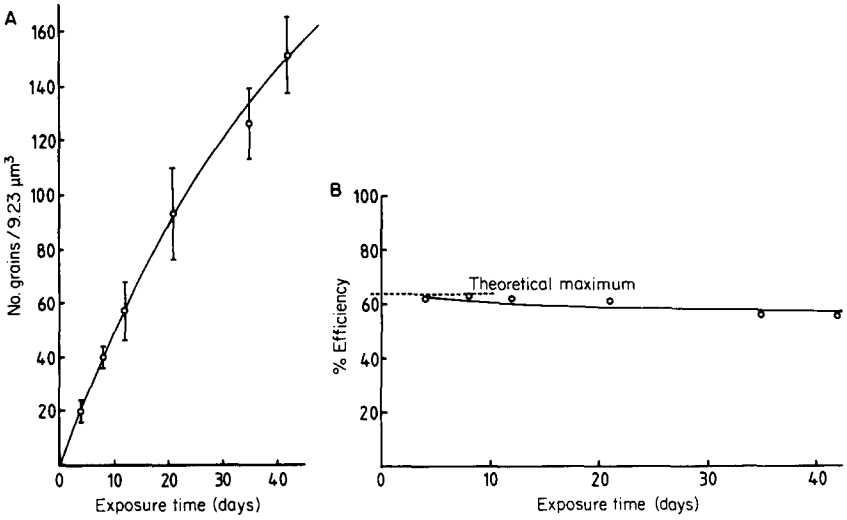

Figure 9. Grain density as a function of exposure time and efficiency of the autoradiographic procedure. Ultrathin sections of embedded ^{125}I-BSA, containing a known amount of radioactivity, were processed for electron microscopic autoradiography and developed in Kodak D-19 after various exposure times (4–42 d). (*A*) The average number of silver grains produced by this fixed amount of labeled material during different exposure periods expressed graphically as a function of time. Note that during the first 3 wk of exposure, the increase in the number of grains produced was linear; the curve only levels off significantly after 30-d exposure time. (*B*) Percent efficiency values were obtained from the total number of disintegrations occurring per unit volume of labeled material during a specified exposure time, given by the following equation (10): $D = D_0 \times 124{,}000\ [1 - e^{-0.01155(t)}]$, where D is the total disintegrations per unit volume during time t, D_0 is the disintegrations per unit volume at the start of exposure, t is the exposure time in days, and the number of grains produced as a result of these decays, as shown here: % efficiency = (No. of grains × 100)/(No. of decays).

Table IV. Densities of Acceptors for ^{125}I-BoNT Types A and B at Murine Nerve Terminals

Concentration of ^{125}I-BoNT	Exposure time	Grain density	Sites/μm^2 plasma membrane
nM	*d*	*per μm^2*	
Type A			
150	7	4.2	157 ± 33
	14	8.3	161 ± 33
	21	11.3	153 ± 31
	28	14.5	153 ± 30
	35	17.5	153 ± 30
	42	18.5	141 ± 28
			average 153 ± 30
35	28	7.5*	150 ± 31
15	28	7.3*	146 ± 30
Type B			
100	11	13.4	623 ± 129
100	11	13.5	631 ± 132

Using the grain-density values obtained for each time point, the experimental value for efficiency (60 and 62% for BoNT A and B, respectively) and the specific radioactivity of BoNT A and B (630 and 1,241 Ci/mmol, respectively), the number of acceptors for each type was calculated as detailed in Materials and Methods. Error in these calculations was determined by an adaptation of the method of Matthews-Bellinger and Salpeter (27).

* The specific radioactivity for the preparation used was 657 Ci/mmol.

nerve terminal membrane and the myelinated axonal membrane of motor neurons.

We thank R. Williams, C. Shone, P. Hambleton, and J. Melling for their help in the purification and radiolabeling of the toxins.

This work was supported by a Medical Research Council studentship (to J. Black) and a grant from the Wellcome Trust.

Received for publication 6 June 1985, and in revised form 3 April 1986.

References

1. Barnard, E. A., J. O. Dolly, C. W. Porter, and E. X. Albuquerque. 1975. The acetylcholine receptor and the ionic conductance modulation system of skeletal muscle. *Exp. Neurobiol.* 48:1–28.

2. Black, J. D., and J. O. Dolly. 1986. Interaction of ^{125}I-labeled botulinum neurotoxin with nerve terminals. II. Autoradiographic evidence for its uptake into motor nerves by acceptor-mediated endocytosis. *J. Cell Biol.* 103:535–544.

3. Deleted in proof.

4. Boroff, D. A., J. del Castillo, W. H. Evoy, and R. A. Steinhardt. 1974. Observations on the action of type A botulinum toxin on frog neuromuscular junctions. *J. Physiol. (Lond.).* 240:227–253.

5. Burgen, A. S. V., F. Dickens, and L. J. Zatman. 1949. The action of botulinum toxin on the neuromuscular junction. *J. Physiol. (Lond.).* 109: 10–24.

6. Cull-Candy, S. G., H. Lundh, and S. Thesleff. 1976. Effects of botulinum toxin on neuromuscular transmission in the rat. *J. Physiol. (Lond.).* 260: 177–203.

7. Dolly, J. O., C. K. Tse, J. D. Black, R. S. Williams, D. Wray, M. Gwilt, P. Hambleton, and J. Melling. 1981. Botulinum neurotoxin type A as a probe for studying neurotransmitter release. *In* Biomedical Aspects of Botulism. G. E. Lewis, editor. Academic Press, Inc., New York. 47–64.

8. Dolly, J. O., J. Black, R. S. Williams, and J. Melling. 1984. Acceptors for botulinum neurotoxin reside on motor nerve terminals and mediate its internalization. *Nature (Lond.).* 307:457–460.

9. Dreyer, F., and A. Schmitt. 1983. Transmitter release in tetanus and botulinum A toxin-poisoned mammalian motor endplates and its dependence on nerve stimulation and temperature. *Pfluegers Arch. Eur. J. Physiol.* 399:228–234.

10. Fertuck, H. C., and M. M. Salpeter. 1974. Sensitivity in electron microscope autoradiography for ^{125}I. *J. Histochem. Cytochem.* 22:80–87.

11. Fertuck, H. C., and M. M. Salpeter. 1976. Quantitation of junctional and extrajunctional acetylcholine receptors by electron microscope autoradiography after ^{125}I-α-bungarotoxin binding at mouse neuromuscular junctions. *J. Cell Biol.* 69:144–158.

12. Grafstein, B., and D. S. Forman. 1980. Intracellular transport in neurons. *Physiol. Rev.* 60:1167–1283.

13. Greenwood, F. C., W. M. Hunter, and J. S. Glover. 1963. The preparation of ^{131}I-labeled human growth hormone of high specific radioactivity. *Biochem. J.* 89:114–123.

14. Gundersen, C. B., B. Katz, and R. Miledi. 1982. The antagonism between botulinum toxin and calcium in motor nerve terminals. *Proc. R. Soc. Lond. B. Biol. Sci.* 216:369–376.

15. Habermann, E. 1974. ^{125}I-labeled neurotoxin from *Clostridium botulinum* A: preparation, binding to synaptosomes and ascent to the spinal cord. *Naunyn-Schmiedeberg's Arch. Pharmacol.* 281:47–56.

16. Hagenah, R., R. Benecke, and H. Wiegand. 1977. Effects of type A botulinum toxin on the cholinergic transmission at spinal Renshaw cells and on the inhibitory action at Ia inhibitory interneurons. *Naunyn-Schmiedeberg's Arch. Pharmacol.* 299:267–272.

17. Hanig, J. P., and C. Lamanna. 1979. Toxicity of botulinum toxin: a stoichiometric model for the locus of its extraordinary potency and persistence at the neuromuscular junction. *J. Theor. Biol.* 77:107–113.

18. Harris, A. J., and R. Miledi. 1971. The effect of type D botulinum toxin on frog neuromuscular junctions. *J. Physiol. (Lond.).* 217:497–515.

19. Hendry, I. A. 1977. The effect of the retrograde axonal transport of nerve growth factor on the morphology of adrenergic neurones. *Brain Res.* 134: 213–223.

20. Heuser, J. E. 1978. Quick-freezing evidence in favour of the vesicular hypothesis. *Trends Neurosci.* 1:80–82.

21. Heuser, J. E., T. S. Reese, and D. M. D. Landis. 1974. Functional changes in frog neuromuscular junctions studied with freeze-fracture. *J. Neurocytol.* 3:109–131.

22. Hirokawa, N., and M. Kitamura. 1975. Localization of radioactive ^{125}I-labelled botulinus toxin at the neuromuscular junction of mouse diaphragm. *Naunyn-Schmiedeberg's Arch. Pharmacol.* 287:107–110.

23. Hirokawa, N., J. E. Heuser, and L. Evans. 1981. Structural evidence that botulinum toxin blocks neuromuscular transmission by impairing the calcium influx that normally accompanies nerve depolarization. *J. Cell Biol.* 88: 160–171.

24. Holtzmann, E. 1971. Cytochemical studies of protein transport in the nervous system. *Phil. Trans. R. Soc. Lond. B. Biol. Sci.* 261:407–421.

25. Holtzmann, E. 1977. The origin and fate of secretory packages, especially synaptic vesicles. *Neuroscience.* 2:327–355.

26. Kelly, A. M., and S. I. Zacks. 1969. The fine structure of motor endplate morphogenesis. *J. Cell Biol.* 42:154–169.

27. Matthews-Bellinger, J., and M. M. Salpeter. 1978. Distribution of acetylcholine receptors at frog neuromuscular junctions with a discussion of some physiological implications. *J. Physiol. (Lond.).* 279:197–213.

28. Olsnes, S., and K. Sandvig. 1983. Entry of toxic proteins into cells. *In* Receptor-mediated endocytosis. P. Cuatrecasas and T. Roth, editors. Chapman and Hall, London. 187–236.

29. Porter, C. W., and E. A. Barnard. 1975. The density of cholinergic receptors at the endplate postsynaptic membrane: ultrastructural studies in two mammalian species. *J. Membrane Biol.* 20:31–49.

30. Price, D. L., J. Griffin, A. Young, K. Peck, and A. Stocks. 1975. Tetanus toxin: direct evidence for retrograde intraaxonal transport. *Science (Wash. DC).* 188:945–947.

31. Pumplin, D. W., and T. S. Reese. 1977. Action of brown widow spider venom and botulinum toxin on the frog neuromuscular junction examined with freeze-fracture technique. *J. Physiol.* 273:443–457.

32. Rogers, A. W. 1979. Techniques of autoradiography. Elsevier, Amsterdam. 387–413.

33. Salpeter, M. M., and L. Bachmann. 1972. Autoradiography. *In* Principles and Techniques of Electron Microscopy, Biological Applications. M. A. Hayat, editor. Van Nostrand Reinhold Co., Inc., New York. 2:221–278.

34. Salpeter, M. M., and M. Szabo. 1972. Sensitivity in electron microscope autoradiography. I. The effect of radiation dose. *J. Histochem. Cytochem.* 20:425–434.

35. Salpeter, M. M., L. Bachmann, and E. E. Salpeter. 1969. Resolution in electron microscope radioautography. *J. Cell Biol.* 41:1–20.

36. Sellin, L. C. 1981. Postsynaptic effect of botulinum toxin at the neuromuscular junction. *In* Biomedical Aspects of Botulism. G. Lewis, editor. Academic Press, Inc., New York. 81–92.

37. Sellin, L. C., S. Thesleff, and B. R. DasGupta. 1983. Different effects of types A and B botulinum toxin on transmitter release at the rat neuromuscular junction. *Acta Physiol. Scand.* 119:127–133.

38. Simpson, L. L. 1980. Kinetic studies on the interaction between botulinum toxin type A and the cholinergic neuromuscular junction. *J. Pharmacol. Exp. Ther.* 212:16–21.

39. Simpson, L. L. 1981. The origin, structure and pharmacological activity of botulinum toxin. *Pharmacol. Rev.* 33:155–188.

40. Small, J. V. 1968. Measurement of section thickness. *4th Eur. Conf. Electron Microsc. (Rome).* 609–610.

41. Sugiyama, H. 1980. *Clostridium botulinum* neurotoxin. *Microbiol. Rev.* 44:420–448.

42. Thesleff, S. 1981. Neurophysiologic aspects of botulinum poisoning. *In* Biomedical Aspects of Botulism. G. Lewis, editor. Academic Press, Inc., New York. 65–79.

43. Tse, C. K., J. O. Dolly, P. Hambleton, D. Wray, and J. Melling. 1982. Preparation and characterization of homogeneous neurotoxin type A from *Clostridium botulinum*: its inhibitory action on neuronal release of acetylcholine in the absence and presence of β-bungarotoxin. *Eur. J. Biochem.* 122:493–500.

44. Tsuji, S. 1974. On the chemical basis of thiocholine methods for demonstration of acetylcholinesterase activities. *Histochemistry.* 42:99–110.

45. Valtorta, F., L. Madeddu, J. Meldolesi, and B. Ceccarelli. 1984. Specific localization of the α-latrotoxin receptor in the nerve terminal plasma membrane. *J. Cell Biol.* 99:124–132.

46. Williams, R. S., C. K. Tse, J. O. Dolly, P. Hambleton, and J. Melling. 1983. Radioiodination of botulinum neurotoxin type A with retention of biological activity and its binding to brain synaptosomes. *Eur. J. Biochem.* 131: 437–445.

47. Zacks, S. I. 1973. The Motor Endplate. R. E. Krieger Publishing Co., Inc., Melbourne, Florida.